Pergamon

Cement and Concrete Research 30 (2001) 405–412

CEMENT AND CONCRETE RESEARCH

Application of ultrasonic testing to describe the hydration of calcium aluminate cement at the early age

T. Chotard*, N. Gimet-Breart, A. Smith[1] , D. Fargeot, J.P. Bonnet, C. Gault

Groupe d'Etude des Matériaux Hétérogènes (GEMH, JE 2213), Ecole Nationale de Céramique Industrielle, 47 à 73 Avenue Albert Thomas, 87065 Limoges Cedex, France

Received 12 May 2000; accepted 2 October 2000

Abstract

Nondestructive and in situ characterisation techniques, such as ultrasonic measurements, permit to follow cement hydration at the early age from a few minutes to a few hours after mixing. The technique reported in this paper is based on measurements in reflection modes. Results concerning an aluminous cement, Secar71, are presented (water-to-cement weight ratio (W/C): 0.3 and 0.4; temperature of measurement: 20°C; duration: 0–24 h). Information deduced from ultrasonic measurements (longitudinal wave velocity, reflection coefficient) associated with other data obtained from X-ray diffraction (XRD), differential thermal analysis (DTA) and thermogravimetric (TG) measurements enable to propose a qualitative description of hydration's chronology. The sensitivity of these ultrasonic parameters to hydrates formation and structuring is underlined.

Keywords: Hydration; Calcium aluminate cement; Ultrasonic measurement; Mechanical properties

1. Introduction

Calcium aluminate cements are a range of cements in which calcium aluminates are the main phase constituents. These materials are used for many special applications in the construction, civil engineering and refractory industries because of their ability to gain strength rapidly and to withstand aggressive environments and high temperature [1,2]. The knowledge of their mechanical behaviour at a young age becomes essential to forecast their performance in service. In order to describe hydration of cement paste at the early age (from a few minutes to a few hours after mixing), different approaches have been developed. Conductivity and pH measurements, usually carried out on dilute systems, have been applied to predict the dissolution and precipitation processes [3,4]. Classical techniques such as thermal analysis, X-ray diffraction (XRD) and scanning electron microscopy, have also been carried out. These characterisations are done ex situ after stopping hydration [5–8]. Aluminous cements hydration has also been investigated by proton and aluminium nuclear magnetic resonance [9,10] or more recently by neutron diffraction [11,12]. These last two techniques correspond to in situ measurements. In this paper, we wish to present another original in situ technique for looking at hydration of fresh pastes. It is based on ultrasonic testing, which has already proven to be reliable for characterising hard cements [13,14]. Several attempts to detail the growth of structure in fresh cement pastes during the 1 or 2 h after mixing have been reported in the literature [15–24]. They dealt with the component of ultrasonic signal, which is transmitted inside the material. The technique presented in this paper considers both the transmitted and reflected signals. Results reported here refer to Secar71, where characteristics are given in Table 1.

2. Experimental procedure

2.1. Preparation of the cement paste

Two lots of paste have been prepared with a water-to-cement weight ratio (W/C) equal to 0.3 and 0.4. Each lot has

* Corresponding author. Tel.: +33-5-55-45-22-36; fax: +33-5-55-79-09-98.

E-mail addresses: t.chotard@ensci.fr (T. Chotard), a.smith@ensci.fr (A. Smith).

[1] Also corresponding author.

0008-8846/00/$ – see front matter
PII: S0008-8846(00)00446-4

Table 1
Characteristics of Secar 71

Chemical composition	Al_2O_3: 69.8–72.2 wt.% CaO: 26.6–29.2 wt.%
Specific Blaine surface	3800 to 4400 cm^2/g
Average particle size	50 μm
Minimal particle size	1 μm
Maximal particle size	100 μm
Density	2.90–3.05 g/cm^3

been mixed according to the normalised procedure No. CEN 196-3. These lots are noted SE030 and SE040, respectively. After mixing, the paste is poured in polymethylmethacrylate (PMMA) moulds prior to ultrasonic measurements. The removal of air is done under a significantly low pressure for 15 min. The quantity of paste is sufficiently large to avoid a change in W/C during air removal.

2.2. Characterisation techniques

2.2.1. Ultrasonic measurements

These characterisations are carried out at 20°C and 95% relative humidity. Short pulses of acoustic waves are radiated by a source (transducer) with sufficiently low amplitude of vibration for the cement to remain in its viscoelastic or elastic state depending on whether it is a liquid or a solid. Reflection pulse echo technique enables to measure the transit time related to the ultrasonic velocity. In the present case, the experimental setup is designed to operate in a semiinfinite mode (Fig. 1), which means that the dimensions of the tested sample are very large compared to the ultrasonic wavelength. A transducer sends wideband pulses of longitudinal ultrasonic wave with a central frequency of 1 MHz (Panametric), which propagate into a buffer acting as a delay line. Considering the dimensions of the mould (100 × 50 × 10 mm), the average particle size of the cement powder (50 μm) and the average value of the longitudinal wave velocity already measured on set samples (3400 m/s), the value of the central frequency (1 MHz) has been chosen in order to be in accordance with the semi-infinite mode [wavelength (λ) dimensions of the mould] and with the homogeneity of the material [wavelength (λ) average particle size). The longitudinal wave velocity has been measured in the 10-mm direction. The proportion of transmitted wave inside the cement-based material depends on the reflection coefficient at the buffer/cement interface. The transit time, t, through the cement sample is related to its thickness, e, and the velocity of longitudinal wave, V_L (m s^{-1}), as follows [Eq. (1)]

$$V_L = \frac{2e}{t} \tag{1}$$

The experimental error on V_L is of the order of 2%. Measurement of t is obtained according to the procedure described elsewhere [25]. In addition to the ultrasonic measurements, the temperature of the mixture was recorded during the whole experiment by a T-thermocouple immersed in the sample.

Our experimental setup also permits to measure the amplitude, A, of the waves reflected at the buffer/cement interface. The corresponding reflection coefficient, R, is related to the acoustic impedances (in kg m^{-2} s^{-1}) of the two materials, namely the cement (Z_{cement}) and the buffer (Z_{buffer}), by the following relation

$$R = \frac{Z_{cement} - Z_{buffer}}{Z_{cement} + Z_{buffer}} \tag{2}$$

For the present study, the buffer is made of PMMA, which has an acoustic impedance close to that of cement when it is in the liquid state. The reflection coefficient approach has already been use by Öztürk et al. [26] in order to monitor the setting and hardening of cement-base materials. They used both longitudinal and shear wave reflection factors. This interesting study dealt with Portland mortars with different additives.

By measuring a reference amplitude, noted A_{ref}, for an echo reflected at the interface between the buffer and a medium with a known acoustic impedance, Z_{ref}, the value of R can be deduced by

$$R = \frac{A}{A_{ref}} R_{ref} \tag{3}$$

where R_{ref} is the reflection coefficient at the interface between the buffer and the reference medium with its acoustic impedance, Z_{ref}. R_{ref} is given by Eq. (4)

$$R_{ref} = \frac{Z_{buffer} - Z_{ref}}{Z_{buffer} + Z_{ref}} \tag{4}$$

In our case, the reference medium is air where $Z_{ref} \sim 0$ kg m^{-2} s^{-1}. This gives $R_{ref} \sim 1$ and Eq. (3) becomes $R \sim A/A_{ref.}$. For a perfect interface between the buffer and the cement, the acoustic impedance is related to the velocity by

$$Z_{cement} = \rho V_L \tag{5}$$

where ρ (in kg m^{-3}) refers to the density of the material.

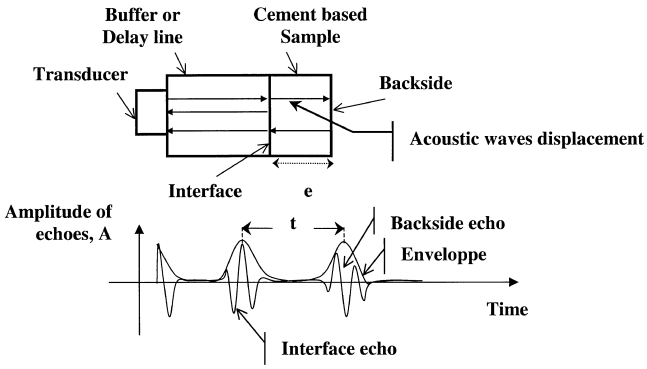

Fig. 1. Schematic representation of the experimental setup for ultrasonic testing.

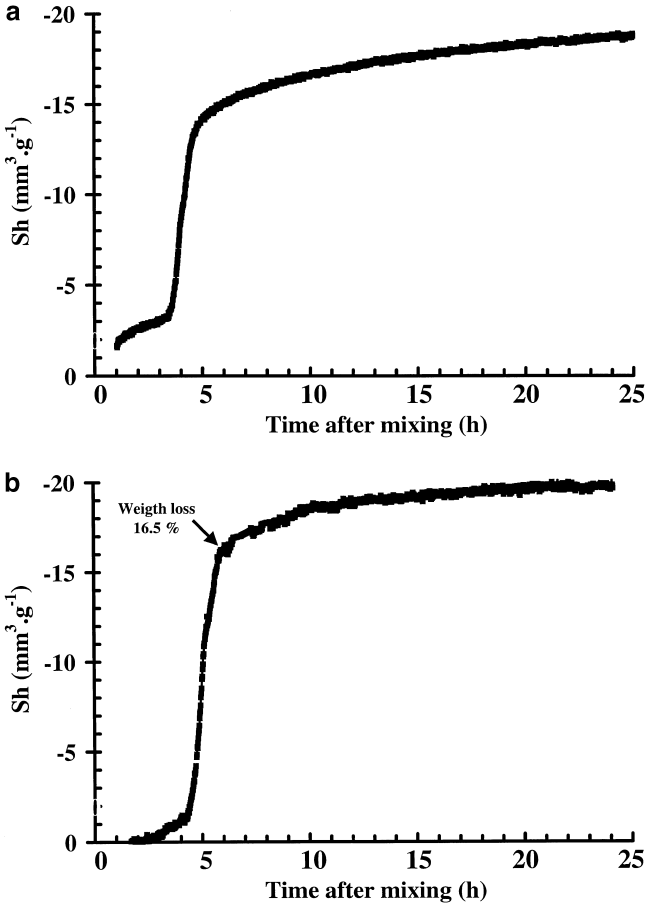

Fig. 2. Sh variations as a function of time for Secar71 mixed with two different W/C ratios. (a) SE030; (b) SE040.

The combination of Eqs. (2) and (5) gives a direct relation between R and ρ. Due to the error on A values (maximum ≈ 5–10%), the precision on R is of the order of 5–10%.

2.2.2. Other measurements

Volume variations during cement hydration have been estimated from Archimede's method. It consists of pouring the paste in a latex membrane just after mixing. The quantity of paste that has been used in the present case is equivalent to the amount poured in the PMMA mould. The sample is supported in water. The apparent weight variations are recorded as a function of time and related to volume changes. Similar procedures have been described in the literature [27–29]. Measurements of volume changes, ΔV (in m^3), correspond to the difference between the volume V_t at $t>0$ s and the initial volume, V_0, at $t=0$ s. The relation between volume changes and Le Chatelier's shrinkage, Sh, normally expressed in $mm^3\ g^{-1}$, is given by Eq. (6) [30]

$$10^{-6} \times \Delta V = \mathrm{Sh} \times m_{\mathrm{cement}} \quad (6)$$

where m_{cement} is the mass of anhydrous cement (in kg).

In our study, on top of these in situ characterisations (namely T, V_L, R and Sh), we have also used other methods for determining the chemical nature of the hydration products. When cement hydration progresses, the material goes from a paste to a solid state. In order to carry out the ex situ characterisation of the formed hydration products, specimens of the cement are taken at increasing times. The cement hydration is stopped by a mixture of ethanol and ether in a 1:1 volume ration [31]. This procedure eliminates the water which is not trapped in hydrates. The resulting product is ground to obtain a powder and characterised by XRD, differential thermal analysis (DTA) and thermogravimetric (TG) measurements. XRD has been conducted with an INEL CPS 120-Curved Position Sensitive diffractometer. Thermal analysis has been carried out with a DTA-TG coupled RIGAKU thermoflex; each experiment has been done on 96 mg of product under dry nitrogen with a heating ramp of 15°C/min. The reference material is a calcined alumina from PROLABO.

3. Results and discussion

In Fig. 2, the variations of Le Chatelier's shrinkage (Sh) for SE030 (Fig. 2a) and SE040 (Fig. 2b) for the paste inside the latex membrane are reported. The time scale corresponds to the duration elapsed after mixing water and cement. In addition, TG measurements have been performed

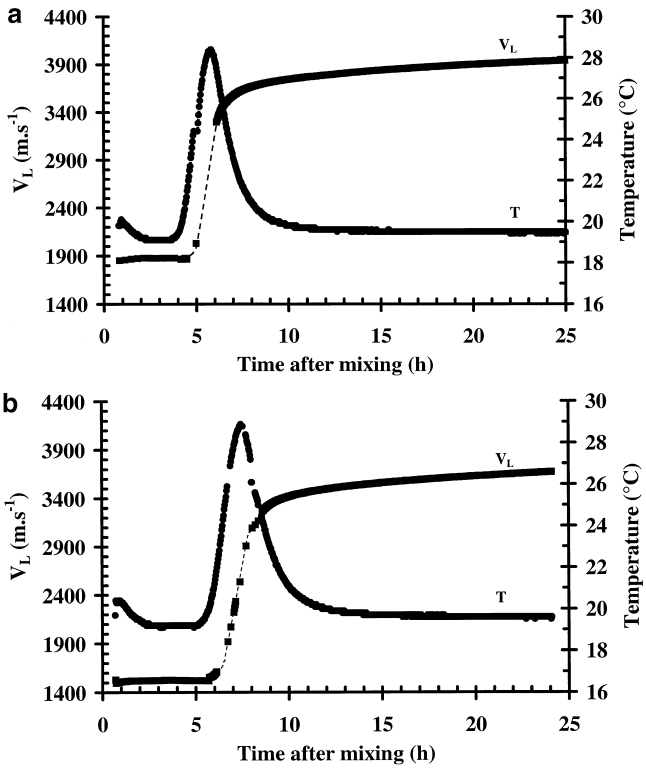

Fig. 3. V_L (■) and T (●) variations as a function of setting time for Secar71 mixed with different W/C ratios. (a) SE030; (b) SE040.

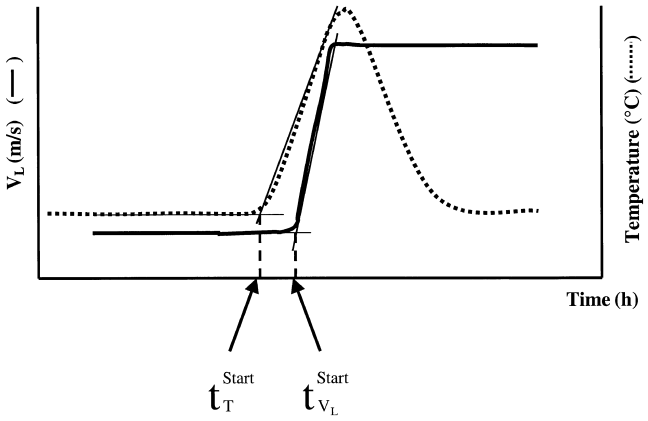

Fig. 4. Schematic representation of V_L and T variations as a function of time. Description of the graphical determination of $t_{V_L}^{Start}$ and t_T^{Start}.

at the end of massive Sh variations. Prior to thermal characterisation, all the free or nonbound water has been removed in the tested samples by solvent exchange. Therefore, TG measurements permit to evaluate the quantity of bound water since the thermal treatment degrades the hydrates. The weight loss has been calculated after heating the samples up to 1000°C. In the case of SE040, the weight loss is equal to 16.5% for Sh equal to 16 mm^3/g (Fig. 2b).

Fig. 3 shows the variations of V_L and T for SE030 (Fig. 3a) and SE040 (Fig. 3b) for the cement contained in the PMMA mould. For each set of data, two characteristic times have been graphically determined as shown in Fig. 4 and are summarised in Table 2. $t_{V_L}^{Start}$ and t_T^{Start} refer to the times when there is a significant modification of slope for V_L and T, respectively. In both cases, before $t_{V_L}^{Start}$, V_L has a low value (1800 m s^{-1} for SE030 and 1500 m s^{-1} for SE040), which is close to the longitudinal wave velocity in water (around 1430 m s^{-1} at 20°C). The slightly larger value obtained in the case of SE030 could be due to the lower quantity of water compared to SE040. After a notable increase, V_L reaches an asymptotic value around 3900 and 3400 m s^{-1} at 24 h for SE030 and SE040, respectively. This difference, which is greater than the experimental error on V_L measurements, can be related to the difference in the available water amount between the two compositions. Concerning the temperature variations, there is a large exothermic phenomenon which starts earlier than the velocity variations $t_{V_L}^{Start} < t_T^{Start}$. In Fig. 5, for SE040 sample, the R coefficient directly deduced from ultrasonic measurements (called R_{exp}) and the R coefficient (called R_{cal}) deduced from the calculated acoustic impedance are plotted

Table 2
Characteristic times for the different tested mixtures

Mix nature	$t_{V_L}^{Start}$	t_T^{Start}
SE030	4 h and 20 min	4 h
SE040	6 h	5 h and 43 min

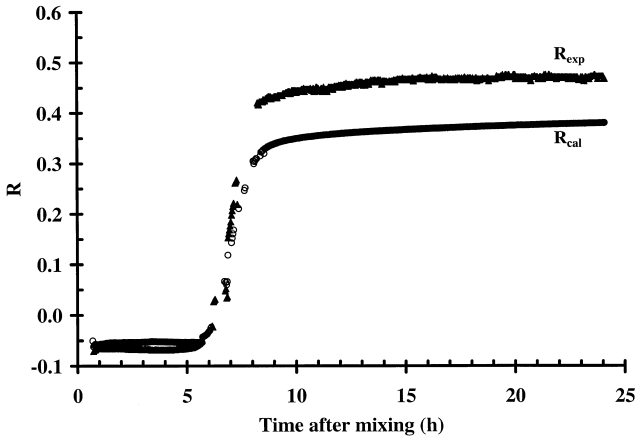

Fig. 5. Variations of R_{exp} (▲) and $R_{cal.}$ (○) as a function of time.

using the following relation [Eq. (7)]

$$Z_{cal} = \rho_{LeChatelier} V_L \quad (7)$$

Where $\rho_{LeChatelier}$ is deduced from hydrostatic measurements. It leads to Eq. (8)

$$R_{cal} = \frac{Z_{cal} - Z_{buffer}}{Z_{cal} + Z_{buffer}} \quad (8)$$

It can be seen in Fig. 5 that the value of both R_{exp} and R_{cal} are closely related during the first 7 h. Beyond this time, R_{exp} is greater than R_{cal}.

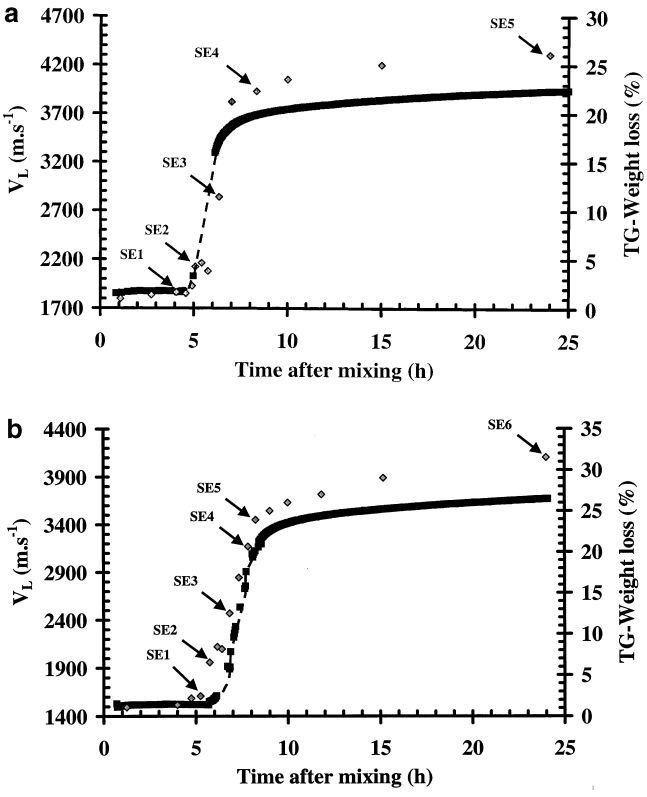

Fig. 6. Weight loss (✦) and longitudinal velocity (■) variations as a function of time for (a) SE030 and (b) SE040.

Since V_L and R are the most interesting data for assessing the mechanical behaviour of the cement, our discussion is mainly focussed on these parameters. In the work of Öztürk et al. [26] on Portland mortars, the evolution of reflection coefficients is compared only with the temperature variations. A good agreement between these two indirect parameters was found by the authors. In addition to our study, for each specimen where hydration has been stopped at chosen times, the weight loss has been calculated from TG measurements. Fig. 6 presents results of V_L and weight losses for SE030 (Fig. 6a) and SE040 (Fig. 6b). By comparing Fig. 6a and b, the observed values of weightlosses for SE040 are greater than the weight losses for SE030. The quantity of formed hydrates increases when the W/C ration changes from 0.3 to 0.4 due to the higher quantity of available water in the mixture. Moreover, it is interesting to note that the weight loss evolution closely follows V_L variations. The corresponding DTA for the same specimens are presented in Fig. 7. The thermal spectra do not show noticeable signals below 4h and 5 min and 5 h and 15 min for SE030 (Fig. 7a) and SE040 (Fig. 7b), respectively. As a matter of fact, even if hydrates are already formed, their amount is probably too low to lead to a detectable heat exchange during their decomposition. Other techniques, such as high frequency measurements on fresh paste between 1 MHz and 1 GHz, permit to identify hydrate formation during this first period [32,33]. The major endothermic peaks recorded afterwards can be attributed to dehydration of CAH_{10}, C_2AH_8 and AH_3 [9,34]. Lastly, Fig. 8 presents XRD spectra for some setting times in the case of SE030 (Fig. 8a) and SE040 (Fig. 8b), respectively. We can see that crystallised calcium aluminate hydrates can be detected only after 6 h and 20 min for SE030 (Fig. 8a) and 7 h for SE040 (Fig. 8b).

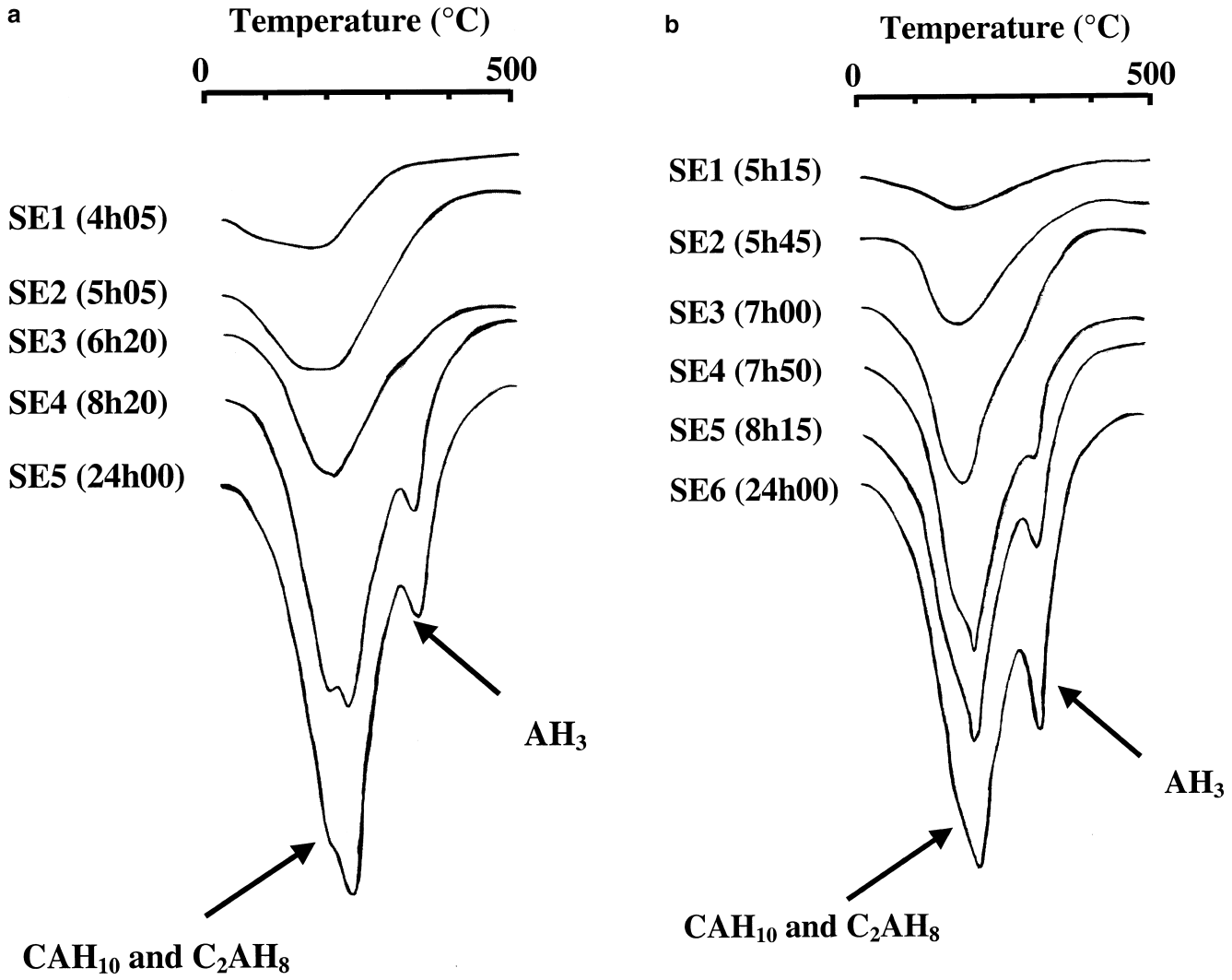

Fig. 7. Thermal analysis for (a) SE030 and (b) SE040 at increasing setting times. These times are numbered according to Fig. 6.

If we compare the evolution of the different sets of data (namely, V_L, T, R, weight loss, DTA and XRD), we can propose the following sequence for cement hydration in a qualitative manner (Fig. 9).

Step 1: The velocity remains low (close to the longitudinal wave velocity in water) and fairly constant while the temperature changes. During this first period, hydrates are probably formed in very low amounts. The ultrasonic waves travel across the water like medium.

Step 2: V_L increases notably, the weight loss of bound water (measured by TG) increases (Fig. 6), which means that the quantity of formed hydrates is growing. During this step, two major events are occurring. The beginning is characterised by Le Chatelier's shrinkage, the grains come closer to each other as hydration proceeds [27]. After several hours (7 h in the case of SE40 for instance), crystallised calcium aluminate hydrates are detected and a difference between R_{exp} and R_{cal} is observed (Fig. 5). These experimental facts suggest in such heterogeneous samples that R_{exp} is not only sensitive to relative density variations but also to modification in the material structure. In addition, by comparing weight losses at the end of massive variation of Sh and V_L, which are reported respectively in Figs. 2 and 6, we can notice that variation of R_{exp} is also sensitive to the quantity of formed hydrates. A study is in progress to better understand the existing relationship between R_{exp} variations and microstructural changes at constant apparent relative density in such a heterogeneous material. When the structure has certain stiffness, water seems to be no longer the major propagation medium for the ultrasonic waves. Schematically and qualitatively [35], the volume changes, which take place during Step 2, are represented in Fig. 10.

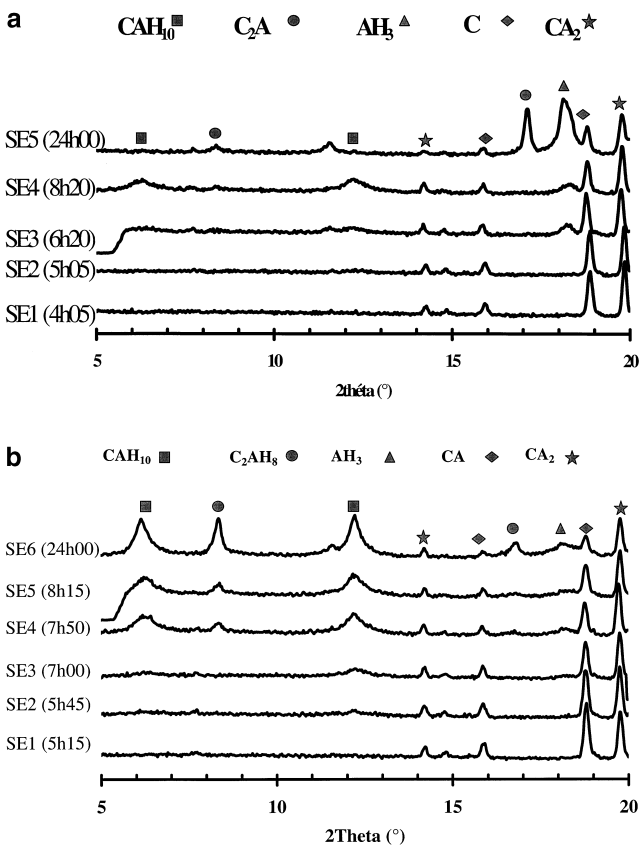

Fig. 8. XRD spectra for (a) SE030 and (b) SE040 at increasing setting times. These times are numbered according to Fig. 6. For the most significant peaks, the chemical nature of the corresponding product is indicated.

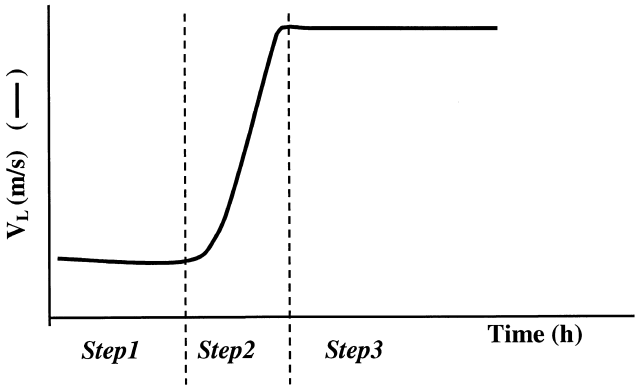

Fig. 9. Main steps of cement hydration.

Step 3: During this stage, the augmentation of V_L is notably reduced. V_L seems to reach an asymptotic value, which is close to the V_L value for solid cement [9].

4. Conclusion

This paper describes ultrasonic testing carried out on Secar71 cement paste just after mixing (W/C = 0.3 and 0.4; temperature of measurement = 20°C). Three parameters are measured in situ, namely the ultrasonic longitudinal wave velocity (V_L), the reflection coefficient (R) and the temperature (T). Their variations as a function of setting time together with information deduced from other ex situ techniques (XRD, DTA and TG), enable to propose a phenomenological description of the hydration process. Three steps can be distinguished.

(i) Step 1: Beginning of hydrate formation.
(ii) Step 2: Le Chatelier's shrinkage and massive precipitation of hydrates with a progressive transition from amorphous to crystallised forms (underlined by the value of R). The mixture stiffens, which corresponds to a major variation of ultrasonic parameters (V_L and R).
(iii) Step 3: The cement skeleton approaches its final stiffness. Therefore, V_L and R evolve only slightly.

Several advantages could be found in this ultrasonic technique:

(i) It is an in situ technique for following the stiffening of the cement paste at a young age through V_L variations.

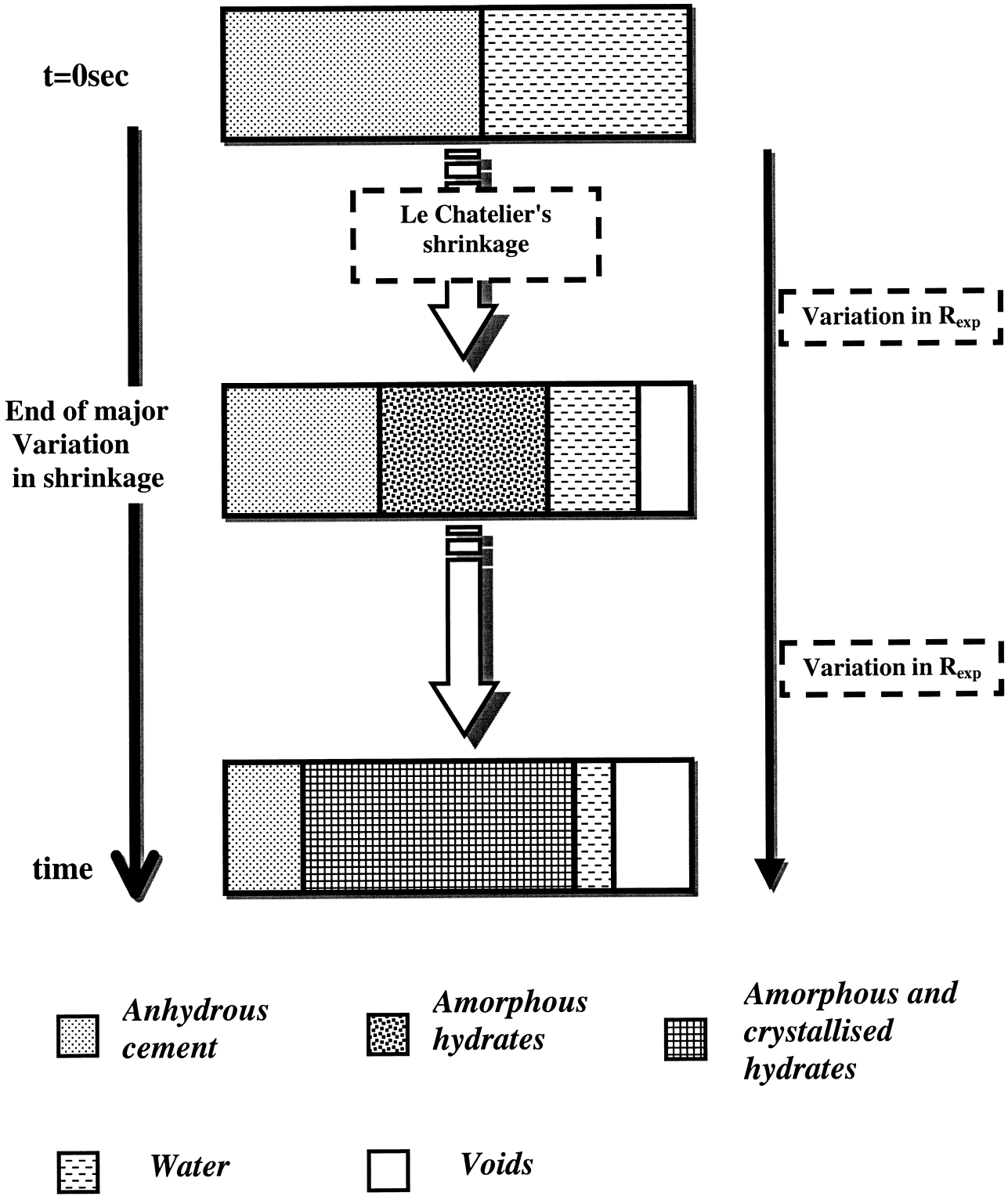

Fig. 10. Schematic representation of the Step 2 chronology.

(ii) It gives in real time information about the evolution of the amount and the structure of formed hydrates, through R variations, inside a material that has reached a certain stiffness.

(iii) The close correlation obtained between the results of this technique and other ex situ measurements clearly shows that, in a near future, ultrasonic measurements may replace other setting tests.

(iv) This technique can be applied at temperatures lower or higher than 20°C in order to evaluate in situ the effect of this parameter on cement setting.

References

[1] K.L. Scrivener, J.L. Cabiron, R. Letourneux, High-performance concretes from calcium aluminate cements, Cem. Concr. Res. 29 (1999) 1215–1223.

[2] H.G. Midgley, in: R.J. Mangabhai (Ed.), Calcium Aluminate Cements, Chapman & Hall, London, 1990, pp. 1–13.

[3] S.P. Jiang, J.C. Mutin, A. Nonat, Studies on mechanism and physicochemical parameters at the origin of the cement setting: I. The fundamental processes involved during the cement setting, Cem. Concr. Res. 25 (4) (1995) 779–789.

[4] A. Capmas, D. Menetrier-Sorrentino, D. Damidot, Effect of temperature on setting times of calcium aluminate cements, in: R.J. Mangabhai (Ed.), Calcium Aluminate Cements, Chapman & Hall, London, 1990, pp. 65–80.

[5] J.H. Sharp, S.M. Bushnell-Watson, D.R. Payne, The effect of admixtures on the hydration of refractory calcium aluminate cements, in: R.J. Mangabhai (Ed.), Calcium Aluminate Cements, Chapman & Hall, London, 1990, pp. 127–141.

[6] K.L. Scrivener, H.F.W. Taylor, Microstructural development in pastes of calcium aluminate cement, in: R.J. Mangabhai (Ed.), Calcium Aluminate Cements, Chapman & Hall, London, 1990, pp. 41–51.

[7] B. Cottin, Etude au microscope électronique de pâtes de ciment alumineux hydratées en C_2AH_8 et CAH_{10}, Cem. Concr. Res. 1 (2) (1971) 177–186.

[8] S. Chatterjiand, A.J. Majumdar, Studies of the early stages of paste hydration of high alumina cements: I. Hydration of individual aluminates, Ind. Concr. J. (1966) 51–55.

[9] N. Richard, Structure et propriétés élastiques des phases cimentières de mono-aluminate de calcium, Thèse de doctorat, Université Paris VI, 1996.

[10] D.J. Greenslade, D.J. Williamson, The use of nuclear magnetic resonance (NMR) in the study of high alumina cement hydration, in: R.J. Mangabhai (Ed.), Calcium Aluminate Cements, Chapman & Hall, London, 1990, pp. 81–95.

[11] S. Rashid, X. Turrillas, Hydration kinetics of $CaAl_2O_4$ using synchrotron energy-dispersive diffraction, Thermochim. Acta 302 (1997) 25–34.

[12] P. Barnes, S.M. Clark, D. Hausermann, E. Henderson, C.H. Fentiman, M.N. Muhamad, S. Rashid, Time-resolved studies of the early hydration of cements using synchrotron energy-dispersive diffraction, Phase Transitions 39 (1992) 117–128.

[13] P.J.M. Monteiro, M.S. King, Experimental studies of elastic wave propagation in high-strength mortar, Am. Ceram. Soc. Testing Mater. (1998) 68–74.

[14] A.H. Harker, P. Schofield, B.P. Stimpson, R.G. Taylor, J.A.G. Temple, Ultrasonic propagation in slurries, Ultrasonics 29 (1991) 427–438.

[15] C.M. Sayers, R.L. Grenfell, Ultrasonic propagation through hydrating cement, Ultrasonics 31 (3) (1993) 147–153.

[16] C.M. Sayers, A. Dahlin, Propagation of ultrasound through hydrating cement pastes at early times, Adv. Cem. Based Mater. 1 (1993) 12–21.

[17] G. Cannard, G. Orcel, J. Prost, Le suivi de la prise des ciments par ultrasons, Bull. Liaison Lab. Ponts Chaussees 168 (1990) 89–95.

[18] J. Keating, D.J. Hannant, A.P. Hibbert, Correlation between cube strength, ultrasonic pulse velocity and volume change for oil well cement slurries, Cem. Concr. Res. 19 (5) (1989) 715–726.

[19] J. Keating, D.J. Hannant, A.P. Hibbert, Comparison of shear modulus and pulse velocity techniques to measure the build-up of structure in fresh cement pastes used in oil well cementing, Cem. Concr. Res. 19 (4) (1989) 554–566.

[20] L. Belkheiri, M. Bocquet, M.L. Abidi, M. Zoukaghe, Continuous ultrasonic measurements during setting and hardening of building materials, Mater. Struct. 32 (1999) 59–62.

[21] S. Labouret, I. Looten-Baquet, C. Bruneel, J. Frohly, Ultrasound method for monitoring rheology properties evolution of cement, Ultrasonics 36 (1998) 205–208.

[22] S. Popovics, J.S. Popovics, Ultrasonic testing to determine water-cement ratio for freshly mixed concrete, Cem. Concr. Aggregates 20 (2) (1998) 262–268.

[23] J. Stepisnik, M. Lukac, Measurement of cement hydration by ultrasonics, Ceram. Bull. 60 (4) (1981) 481–483.

[24] A. Boumiz, C. Vernet, F. Tenoudji Cohen, Mechanical properties of cement pastes and mortars at early ages, Adv. Cem. Based Mater. 3 (1996) 94–106.

[25] T. Cutard, D. Fargeot, C. Gault, M. Huger, Time delay and phase shift measurement for ultrasonic pulses using autocorrelation methods, J. Appl. Phys. 75 (4) (1994) 1909–1913.

[26] T. Öztürk, J. Rapoport, J.S. Popovics, S.P. Shah, Monitoring the setting and hardening of cement-based materials with ultrasound, Concr. Sci. Eng. 1 (1999) 83–91.

[27] G.D. de Hass, P.C. Kreijger, E.M.M.G. Niel, J.C. Slagter, H.N. Stein, E.M. Theissing, M. Wallendael, The shrinkage of hardening cement paste and mortar, Cem. Concr. Res. 5 (4) (1975) 295–320.

[28] J.F. Raffle, Volume changes during hydration of cements and plasters, Br. Ceram. Soc. Proc. 35 (1984) 295–303.

[29] E. Tazawa, S. Miayazawa, T. Kasai, Chemical shrinkage and autogenous shrinkage of hydrating cement paste, Cem. Concr. Res. 25 (1995) 288–292.

[30] R. Dupain, R. Lanchon, J.C. Saint-Arroman, Granulats, sols, ciments, bétons: caractérisation des matériaux de laboratoire, Casteilla, Paris, 1995, pp. 115–121.

[31] A. Bachiorrini, B. Guilhot, Premières échéances de l'hydration de l'aluminate monocalcique: influence du protocole de stoppage, Cem. Concr. Res. 12 (5) (1982) 557–567.

[32] A. Smith, J.P. Bonnet, P. Abelard, Ph. Blanchart, Electrical characterisation of aluminous cement at the early age in the 10 Hz–1 GHz frequency range, Cem. Concr. Res. (in press).

[33] T. Chotard, N. Gimet-Bréart, A. Smith, Y. El Hafiane, J.P. Bonnet, P. Abelard, B. Tanouti, Ph. Blanchard, Electrical characterization at high frequency (1 MHz–1 GHz) of an aluminous cement, Annales de chimie, sciences des matériaux (in press).

[34] M. Murat, Stabilité thermique des aluminates de calcium hydratés et phases apparentées. caractérisation par les méthodes thermoanalytiques, Congrès de Turin. (1982) 59–84.

[35] A.M. Neuville, Properties of Concrete, fourth ed., Longman, London, 1996, pp. 26–31.